

Published in final edited form as:

Nat Protoc. 2008 ; 3(5): 866–876. doi:10.1038/nprot.2008.51.

## L-Measure: a Web-accessible tool for the analysis, comparison, and search of digital reconstructions of neuronal morphologies

Ruggero Scorcioni<sup>1,#</sup>, Sridevi Polavaram<sup>1,2,#</sup>, and Giorgio A. Ascoli<sup>1,2,3,\*</sup>

<sup>1</sup>Krasnow Institute for Advanced Study, George Mason University, Fairfax, Virginia 22030 (USA)

<sup>2</sup>Neuroscience Program, George Mason University, Fairfax, Virginia 22030 (USA)

<sup>3</sup>Department of Molecular Neuroscience, George Mason University, Fairfax, Virginia 22030 (USA)

### Abstract

L-Measure (LM) is a freely available software tool for the quantitative characterization of neuronal morphology. LM computes a large number of neuroanatomical parameters from 3D digital reconstruction files starting from and combining a set of core metrics. After more than six years of development and use in the neuroscience community, LM enables the execution of commonly adopted analyses as well as of more advanced functions. This report illustrates several LM protocols: (a) extraction of basic morphological parameters, (b) computation of frequency distributions, (c) measurements from user-specified sub regions of the neuronal arbors, (d) statistical comparison between two groups of cells, and (e) filtered selections and searches from collections of neurons based on any boolean combination of the available morphometric measures. These functionalities are easily accessed and deployed through a user-friendly graphical interface, and typically execute within few minutes on a set of ~20 neurons. The tool is available at <http://krasnow.gmu.edu/cn3> for either online use on any Java-enabled browser and platform, or download for local execution under Windows and Linux.

### Keywords

axon; branching; dendrite; morphometry; neuroanatomy; software tool; statistics

## INTRODUCTION

The quantitative characterization of neuronal morphology is essential to correlate structure, activity, and function in the nervous system at the cellular level. In many studies, dendrites and axons imaged from a variety of histological preparations are digitally traced into 3D reconstructions representing the arborization as a series of interconnected tubules<sup>1</sup>. These data files allow comprehensive morphometric investigations, powerful comparative analyses, and the implementation of anatomically detailed computational models<sup>2–6</sup>. Digital reconstruction of neuronal morphologies requires specialized software, such as the popular Microbrightfield NeuroLucida. Despite ongoing progress in automation attempts, the tracing

\*Corresponding Author: [ascoli@gmu.edu](mailto:ascoli@gmu.edu), Phone number: 703-993-4383, Fax number: 703-993-4325.

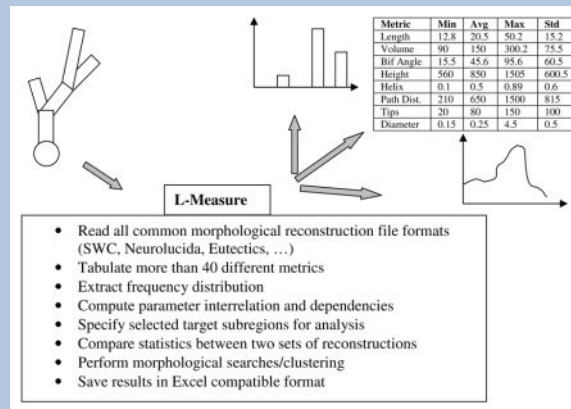
#These authors contributed equally to this work.

process remains extremely time-consuming and technically challenging<sup>7</sup>. At the same time, digital morphologies are extremely versatile, and retain considerable scientific utility beyond the original purpose they are collected for. They can often be re-used in follow-up or even completely unrelated research projects<sup>8</sup>. An increasing number of laboratories are freely sharing their 3D reconstructions with the neuroscience community to maximize the impact of their research efforts<sup>9–14</sup>. Thousands of neurons are available at NeuroMorpho.Org, and hundreds are downloaded daily. Examples of these neuronal morphologies are illustrated in Figure 1.

In order to capitalize on the value of these digital data, we developed and freely distributed L-Measure (LM), a software program to extract morphometric measurements<sup>15</sup>. With more than six years of public usage, LM remains the only documented, supported, and freeware tool available online for the neuroscience community to routinely analyze dendritic and axonal morphologies from digital reconstruction files in any of the known file formats. LM measures a battery of over 40 core metric functions (e.g. diameter, length, angles) and can return simple statistics (average, standard deviation, minimum, maximum, and total sum), histogram distributions, or the dependency of one metric on another (e.g. Sholl analysis of number of branches vs. distance from soma). The same functions can also be used to select a specific portion of the arborization for analysis (e.g. at least 5 bifurcations away from the soma). The underlying C++ computational engine, dedicated to file processing and number crunching, can be operated through a “point and click” Java graphical user interface (or via command line for batch execution). LM outputs are visualized on the display and/or saved to files compatible with analysis and graphic programs such as Microsoft Excel. The core LM functionality is depicted in Box 1.

### Box 1

#### Quantitative morphometry by L-Measure



Since its first introduction in 2001, LM has been proven useful in several applications.

- LM is regularly used for large-scale extraction of morphometrics employed by the online electronic repository NeuroMorpho.Org<sup>16</sup> to characterize the structural content of thousands of 3D digital reconstructions from a variety of cell classes,

anatomical locations, experimental procedures, animal species, and reconstruction methods. In particular, LM is utilized whenever the underlying database is updated and at every version release of NeuroMorpho.Org.

- b. LM is routinely used by several research groups worldwide to perform detailed comparative analysis on groups of neurons. Classic examples of such applications from the authors' own studies and collaborations include the quantification of characteristic morphological features across various cell classes and conditions<sup>17</sup>, detection of differences induced by specific growth factor<sup>18</sup>, analysis of developmental changes<sup>19</sup>, and comparison between neurons expressing various neuropeptides<sup>20</sup>.
- c. Thanks to its capability of processing assorted file formats from diverse reconstruction techniques, LM is also used to match morphologies obtained from multiple digital tracing methods both at the detailed branch-by-branch level and with overall statistics<sup>21</sup>. By the same token, LM has served validation purposes in processing the results of automated reconstruction algorithms applied to projection axons in the rat hippocampus neurons (i.e. comparing number of bifurcations, total length, path distance, branch order, and asymmetry with the same metrics extracted from other available morphologies of the same classes<sup>22</sup>).
- d. LM is also employed for the extraction of parameter distributions from experimental data required for resampling by stochastic computational simulations to generate virtual neurons<sup>23</sup>. Similarly, LM is often used to investigate the quality and limitations of these models by comparing their emergent morphological properties with the original experimental data<sup>24</sup>.

LM is well recognized as a standard tool for morphometric analysis as cited by independent laboratories in a variety of settings, such as the description of computational protocols<sup>25</sup>, database and information frameworks<sup>26</sup>, classification of disease-induced dendritic damage<sup>27</sup>, assessing morphological simulations in spinal injury models<sup>28</sup>, and analysis of experimental manipulations<sup>29</sup>. Moreover, it is important to stress that LM provides the ability to extract all morphological measurements underlying the emerging community standards for classification of cellular phenotypes<sup>30</sup>.

As a “quick start” practical guide of LM functionality, this protocol presents several common procedures illustrating the tool in action. These user case examples are chosen to cover a variety of key operations and the reader is encouraged to try them as an opportunity to explore both basic and new features.

### User Operation of L-Measure

We first provide a brief overview of the LM “look and feel” from a user perspective. Although for the sake of precision we refer specifically to the online version accessed with Internet Explorer under Windows XP (the most popular configuration to date), other platforms and the local executables only differ subtly from this description (to set up LM on a local computer, refer to Box 2).

**Box 2****Setting up L-Measure in seven easy steps**

1. Go to <http://krasnow.gmu.edu/cn3>
2. Click on Data/Tools++ tab
3. Select the L-Measure link
4. Of the two downloadable archives for installing LM, choose the appropriate one corresponding to your operating system (Linux or Windows)
5. Download the Lm.zip file, which contains:
  - LM.exe – a C++ executable engine
  - Lm.jar – a Java based graphical user interface that send point and click commands to the executable engine
6. Extract the Lm.zip content on your local machine, ensuring that both LM.exe and Lm.jar reside inside the same directory
7. Double click on Lm.jar to start the GUI interface

Total time estimate (steps 1–7): 1–2 minutes

From (<http://krasnow.gmu.edu/cn3>), LM loads upon selecting “L-Measure” from the “Data/Tools++” page, and clicking on “Online version”. LM appears as a user-friendly graphical interface with seven tabs that can be inter-toggled by a single mouse click (Figure 2). In particular, the *help* page (rightmost tab) contains an introductory manual and the reference list of available measurements, each with a brief explanation. Several of the remaining tabs are normally accessed in rapid sequence, as described in more details in the “Use Case Examples” below. The typical user delimits the morphological region to which the measurements should be restricted (*specificity*), selects the parameters to be extracted (*function*), loads one or more neurons (*input*), defines how to display or save the results (*output*), and finally launches the analysis (*go*).

All morphological measurements in LM are derived from a core set of metric functions, the majority of which are listed in Table 1. These functions generally extract a measure from each tracing point. In a physical interpretation, these individual points define the ending of each of the interconnected tubular primitives constituting the digital morphology. A subset of these points corresponds to the topological nodes of the trees, i.e. stems (tubules attached to the soma), bifurcations (tubules with two daughters), and terminal tips (tubules without daughters). After parsing the whole neuronal arborization (or the portion delimited by the *specificity* settings), LM can derive three types of relations from the raw values of the measures. The first is a simple statistical summary consisting of mean, standard deviation, minimum, maximum, and the total sum (for examples, see Table 2 for tabulated values and Figure 3a for a scatter plot obtained from these kinds of data). The second is the frequency distribution histogram, with user-defined bins (illustrated e.g. in the inset of Figure 3a). The

third is the interrelation between two measures, also binned by the user, as in the examples of Figure 3b–d.

Individual elements of the statistical summary, applied to appropriate functions, yield useful scalar metrics to characterize overall neuronal structure. For example, the maximum Euclidian distance from soma provides a measure of the neuronal size corresponding to the radius of the smallest sphere containing the neuron. The total sum of the distance from previous point is another metric for the extent of the neuron, its overall cable length. A few functions are direct features of the whole cell, such as somatic surface, or the height, width, and depth of the neuron (comprising all of its trees). Several other functions are not defined for every tracing point, but only at the level of branches (right column in Table 1), i.e. the portions of the arbor between two nodes (e.g. the contraction, or ratio between Euclidian and path distance, reflecting neuritic meander), or more specifically at bifurcations (gray shaded background in the right column of Table 1), such as daughter diameter ratio and local amplitude angle. A review of every morphometric function is beyond the scope of the present report. The definitions of all core metrics are available in the LM *help* tab (and this topic is well represented in the scientific literature<sup>29</sup>).

Not all elements of the statistical summary are appropriate for every core function (e.g., the sum of all diameters is of questionable significance), and several measures can be obtained in a redundant fashion (e.g. both the sums over all branch lengths and over distances from previous points return total cable length). Moreover, important metrics can be also obtained by combining other core functions (e.g. surface and volume from length and diameter, etc.). Overall, LM can measure more than one hundred independent and meaningful morphological parameters. Additional measures can be extracted by *specificity*, by usage of histogram distributions, and by interrelating variables. Analyses can be carried out on entire populations of cells, on individual neurons, and on portions thereof. The resulting outputs can be further manipulated for more extensive post-processing or graphical rendering (as displayed in Figure 3).

### New Available Functionalities

We have recently upgraded LM to include three new features. The first one allows users to test for statistical differences between two groups of neurons, as often performed in neuroanatomical comparisons of an experimental and a control condition (e.g. knock-out vs. wildtype, treated vs. saline, lesioned vs. sham, aged vs. young). The user can load cells in each of the two groups individually and/or selecting entire directories (Figure 4). The parameters to use in the statistics are then chosen from the core functions by selecting the appropriate elements of the statistical summary (Figure 5). The second provides the ability to search large directories of digital reconstructions (e.g. from a series of experiments, or downloaded from an archive) for cells matching specific morphometric criteria (e.g. with less than 20 terminal tips) as shown in Figure 6. The third enables morphological analyses at the individual tree level, i.e. grouping measurements tree-by-tree (each separate part of the arborization that stems directly from the soma) as opposed to an entire cell or set of neurons.

## Potential Applications of L-Measure

Several of the functionalities implemented in LM were inspired by published scientific studies in which important morphometric analyses were performed by hand, or with custom made (and not publicly available) routines. These and many other such reports serve as convincing demonstrations of the research applications for which LM can provide a fast and reliable solution. A recurring theme is the comparative morphological analysis of sets of cells identified or separated by (in principle) independent means. This is a particularly active area of research with respect to GABAergic cells in the cerebral cortex, which are known for their rich diversity. Examples from the adult rat hippocampus alone include the comparison of total dendritic length and soma surface area among three groups of CA1 interneurons identified on the basis of specific chemical markers<sup>32</sup>, and the extraction of similar metrics from dentate gyrus cells characterized by their electrophysiological properties<sup>33</sup>. The issue of cellular classification represents a fundamental scientific question in its own merit, and the extensive battery of measures that are available in LM lends itself to quantitative clustering methods. This kind of strategy was recently used e.g. on the axonal arborizations of interneurons from the monkey prefrontal cortex<sup>34</sup>, and from the mouse visual cortex<sup>35</sup>. Alternative classification approaches, also involving large-scale morphometric extraction, were successfully applied to retinal cells in both mammals<sup>36</sup> and inframammals<sup>37</sup>. In some cases, clustering was adopted in later refinements<sup>38</sup>. More generally, morphometric analysis is prominently used in neuronal classification, as recently exemplified by the distinction of von Economo and pyramidal neurons from human postmortem brains based on branching and symmetry<sup>39</sup>, or the characterization of speech-specific dendritic features from interhemispheric comparison of magnopyramidal cells<sup>40</sup>. Even when interneuron populations display a continuum of morphological properties, and are thus not amenable to classification clustering, principal component analysis over an extensive battery of morphometric measures may reveal functionally relevant anatomical features such as laminar gradients, as in the cerebellar molecular layer<sup>41</sup>.

Another important line of studies investigates how electrophysiological activity, action potential propagation, and neuronal firing dynamics can be modulated by specific morphological parameters, such as the dendritic surface<sup>42</sup> and dendritic branching patterns both among different cell types<sup>43</sup> and within a single class<sup>44</sup>. Other typical examples include the relation between morphometric distributions that can be easily extracted from LM output and the electrotonic structure of the dendrites (e.g. comparing multiple classes of principal and inhibitory cells in the cat spinal cord<sup>45</sup>). In some cases, the morphometric changes may be linked to the expression of growth factors activated during development. For example, it was shown that the number of dendritic terminal tips and total dendritic length were both regulated by the  $\beta$ -catenin complex during morphogenesis<sup>46</sup>. Interestingly, later deployment of LM on this same experimental preparation enabled more comprehensive studies of absolute and relative effects of  $\beta$ -catenin as well as its effect on simulated spiking patterns<sup>18</sup>. Changes in plasticity and neuronal morphology are often observed during development and aging, as well as in disease (Alzheimer's, Parkinson's, etc.), and in a variety of experimental conditions. Illustrations of typical potential uses of LM in these cases are offered by reports on the contrasting stress-induced alterations of the distributions of the number of branch points against Euclidean distance in apical vs. basal dendrites<sup>47</sup>. The changes that occur in

spatial distribution of branch points and terminal tips with normal animal experience have been similarly compared<sup>48</sup>. LM enables these analysis as well as variations that may be more straightforward to interpret biologically, such as the pattern of dendritic surface (instead of branch counts), which relates to synapse numbers, as a function of the more “physiological” path (as opposed to Euclidean) distance. Last but not least, morphometric parameters are routinely analyzed in the course of computational simulations of dendritic structure, as recently applied to the analysis of the relationship between path and Euclidean distance in spinal motoneurons<sup>49</sup>. All the above examples and results could be suitably replicated with LM.

### L-Measure Limitations

Neuronal morphology can be represented and quantified at several levels. The “vector-based” representation of branching structures adopted by most 3D digital reconstruction systems constrains the type of processing enabled by LM. In particular, surface shape analysis and spine or ultra structural metrics are excluded from this type of analysis. Other tools, such as 3DMA<sup>50</sup> offer a complementary solution from this point of view, allowing automated segmentation and 3D voxel analyses from a stack of images. More generally, although LM provides an extensive (and continuously growing) set of metric, the number of measurable geometric characteristics is practically infinite, so it is unavoidable that some users may be interested in specific analyses that are not (yet) implemented. An alternative commercial product, MicroBrightField’s NeuroExplorer ([www.mbfbioscience.com](http://www.mbfbioscience.com)) can be chosen to perform analyses based on terminal distance, convex-hull, or polar histograms. Moreover, LM is restricted to a purely morphometric domain, and does not allow the direct estimation or modeling of functional characteristics, such as eletrotonic structure or electrical impedence. Thus, the additional use of external simulation environment such as NEURON ([www.neuron.yale.edu](http://www.neuron.yale.edu)) to investigate the relationship between morphological and electrophysiological properties<sup>6,17,33</sup> is required. However, none of these software applications (3DMA, NeuroExplorer, or NEURON) enables any of the key LM advantages, such as the extensive and unique list of available metrics, the flexibility to access the tool both online and as standalone application, the direct statistical comparison between and/or search within cell groups, and the morphological specification of subparts of neuronal structures.

### Step-by-Step Use Case Examples

The procedure detailed below describes a set of representative morphometric analyses. In particular, after a preliminary step of data preparation (A), the protocol illustrates the extraction of total length, surface, and volume data (B). These are standard scalar parameters that quantify various aspects of the neuronal arbor size. Next (C) is the derivation of the histogram distribution of branch length, i.e. the frequency of distances between consecutive bifurcations or between a bifurcation and a termination along the neural path. This metric provides an assessment of the local variability at the branch level within the neuronal population. The following two cases (D and E) characterize the interrelations between surface area and relative path distance, and between number of internal basal branches and branch order, respectively. These are powerful variations of the classic “Sholl analysis”, which was originally introduced to capture the branching patterns as a function of the cell

spatial surroundings<sup>51</sup>. Sholl plots were defined before the digital era based on the available pencil tracings on paper, as the number of branches intersecting a series of concentric circles versus the radii of the circles. The use of path (instead of radial) distance provides a more natural and “cell-centric” perspective, and also captures the full three-dimensional spatial extent as opposed to a planar projection. The choice of a “relative” coordinate system (essentially normalizing the path to the maximum distance from soma to tips) enables the comparison of trees with very different sizes. Moreover, switching the dependent variable to surface area (from number of branches) enhances the functional relevance of the analysis by reporting a measure related to the neuronal electrotonic structure and the number of synapses. The selection of “internal” branches seamlessly instantiates a further important distinction by including in the analysis bifurcating branches and excluding terminating ones. Finally, the remaining set of user cases exemplifies other aspects of the functionality available in LM. One case (F) consists of the statistical comparison of two sets of neurons based on their total length, total surface, and mean branch order. Another (G) searches and finds within a large data set all the neurons with volume greater than 2000  $\mu\text{m}^3$  and length greater than 18,000  $\mu\text{m}$ . These search results are then pipelined and subjected to statistical analysis (H). The last case (I) tabulates surface area in basal dendrites farther than two bifurcations away from the soma as a function of relative path distance in individual subtrees. These instances are offered as typical usage examples from our practical experience with LM. A large number of additional useful combinations of this functionality provides ample opportunity for other possible morphometric analyses.

## MATERIALS

### EQUIPMENT

- All protocols have been tested on:
  - Intel Pentium IV processor 2.8GHz with 1.5GB of RAM running Windows XP OS for both online and standalone versions;
  - Intel dual quad core processor 2.0GHz with 4GB of RAM running Linux Fedora 7 OS for both online and standalone versions;
  - Intel core duo 2.16GHz processor with 1GB of RAM running Mac OS X for online version only.
- The LM tool can be downloaded and run locally as a standalone application on Windows or Linux machines (for standalone set up on the local hard drive, follow steps in Box 2).
- LM can also be accessed directly on-line with any (Java enabled) Internet browser and operating system. On the server side the requests are served by an Intel dual quad core processor with 4GB of RAM running on Fedora 7 OS. On the client side, protocols were tested on:
  - Internet Explorer and Netscape on Windows XP machines;
  - Mozilla Firefox on Windows and Linux machines; and
  - Safari on Mac machines.



! CRITICAL: For on-line usage, a security prompt asks for reading and writing privileges. Granting this permission by accepting the signed certificate allows LM to read locally stored cells and write the output results on the user's local hard disk.

## PROCEDURE

### (A) Data Preparation

- 1| To run these demonstrations, sets of neurons need to be downloaded from NeuroMorpho.Org. In particular all hippocampal CA1 and CA3 neurons from Amaral's archive are needed. Go to <http://www.NeuroMorpho.Org>, and select "Metadata" under the left side "Search by" menu.
- 2| Click on "Brain Region". Select "Hippocampus" and "CA1" from the dropdown lists.
- 3| Click on "Archive" and choose "Amaral" from the dropdown list.
- 4| Hit the "Show Summary" button and at the bottom of the page click "Select All" and "get SWC files of selected neurons".
- 5| Download the ZIP file and extract its content to "AmaralOrigCA1" folder on the local hard drive.
- 6| Repeat these steps by choosing "Hippocampus" and "CA3" in the Brain Region menu and submenu respectively, and select "Amaral" under Archive. Finally, download the ZIP file and extract its content to "AmaralOrigCA3" folder.
- 7| Continue with all other cases below (B-I).

### (B) Extraction of total dendritic length, surface, and volume data

! CAUTION: Make sure all the windows and checkboxes are reset before switching from one example to another. Use the "Remove All" buttons in the respective panels and uncheck the previously checked options.

- i. In the *Specificity* panel, select *Type* from left list. Press the *Add* button.
- ii. Set = for *Operator*. Input 4 for *Value*. A type equal to 4 in NeuroMorpho.Org corresponds to apical dendrites.
- iii. Select *Type* from the left list. Press the *Add* button.
- iv. For the second row in the left table set OR for *Connector*. Set = for *Operator*. Input 3 for *Value*. A type equal to 3 corresponds to basal dendrites.
- v. In the *Function* panel, select *Volume*, *Length* and *Surface* from the top left list. Multiple functions can be selected by keeping the Ctrl key pressed. Press the *Add* button. All three metrics should now appear in the top right white window (Figure 2).
- vi. In the *Input* panel, click *Add* (top left) and select the c10261.CNG.swc and c11563.CNG.swc neurons from AmaralOrigCA1 folder.

- vii. In the *Go* panel, hitting the *Go* button will result in a display similar to Table 2.

### (C) Histogram distribution of branch length

- i. In the *Specificity* panel, select *Type* from the left most list. Press the *Add* Button.
- ii. Select *Operator* and set it to =. Input 4 in the *Value* cell.
- iii. Select *Type* from the left list and press the *Add* Button.
- iv. For the second row in the left table set OR for *Connector*. Set = for *Operator*. Input 3 for *Value* cell.
- v. In the *Function* panel, select *branch\_pathlength* from both top and bottom left panels. Select *Width of Bins* and set its value to 25. Press the *Add* button.  

! CAUTION: Do not click the *Add* button before entering the value 25 for *Width of Bins*. Otherwise, the default value (of 10) will be assumed by the LM executable.
- vi. In the *Input* panel, click *Add* (top left) and select the *AmaralOrigCA1* folder. Repeat for the *AmaralOrigCA3* folder.
- vii. In the *Output* panel, select the *Global* checkmark.
- viii. In the *Go* panel, hitting the *Go* button will produce the data plotted in the inset of Figure 3a.

### (D) Interrelation between surface area and relative path distance

- i. In the *Specificity* panel, select *Type* from left list. Press the *Add* button.
- ii. Select *Operator* and set it to =. Input 4 for *Value* cell.
- iii. Select *Type* from left list. Press the *Add* button.
- iv. In the *Function* panel, select *Surface* from top left list and *PathDistance* from the bottom left list.
- v. In the *Input* panel, click *Add* (top left) and select the *c10861.CNG.swc* neuron from *AmaralOrigCA3* folder.
- vi. In the *Go* panel, hit the *Go* button to start the measurement process. Figure 3b is generated by executing case D on all *Amaral CA3* neurons, first by selecting only apical dendrites and then by selecting only basal dendrites.

### (E) Interrelation between number of internal basal branches and branch order

- i. In the *Specificity* panel, select *Type* from left list. Press the *Add* button.
- ii. Select *Operator* and set it to =. Input 3 for *Value* cell.
- iii. Select *TerminalSegment* from left list. Press the *Add* button.
- iv. Set *AND* as *Connector* and > as *Operator*. Input 1 for *Value* cell. Values greater than 1 return only internal segments.

- v. In the *Function* panel, select *N\_Branch* from top left list and *Branch\_Order* from bottom left list.
- vi. Select *Width of Bins* checkmark and set its value to *1*. Press the *Add* button.
- vii. In the *Input* panel, click *Add* (top left) and select *c10861.CNG.swc* neuron from *AmaralOrigCA3* folder.
- viii. In the *Go* panel, hit the *Go* button to start the measurement process. The results are displayed in Figure 3c as “Internal C10861”.

**(F) Comparison of two neuron sets based on total length, total surface, and mean branch order**

- i. In the *Specificity* panel, select *Type* from left list and press *Add*.
- ii. Set = as *Operator*. Input *4* for *Value* cell.
- iii. Select *Type* from left list. Press the *Add* button.
- iv. Set *OR* for the second row *Connector*. Set = as *Operator*. Input *3* for *Value* cell.
- v. In *Function*, *Add Length*, *Surface*, and *Branch\_Order*, following the steps outlined in Case B above.
- vi. Mark the *Stat\_tests* box. Of the checkboxes appearing in the top right display (one for each element of the statistical summary), select *Sum* for *Length* and *Surface*, and *Avg* for *Branch\_Order*.
- vii. In the *Input* panel, *Add* all neurons of the CA1 group by selecting the *AmaralOrigCA1* directory as *Group1*.
- viii. Check the *Stat\_tests* box and *Add* all neurons of the CA3 group by selecting the *AmaralOrigCA3* folder as *Group2*.
- ix. In the *Tests* options at the bottom of the panel, choose *Wilcoxon* test and among the *Corrections* choose *Bonferroni*.
- x. Executing the analysis in the *Go* panel by clicking on the *Go* button will yield the (self-explanatory) results in Table 3.

**(G) Finding neurons with volume greater than 2000  $\mu\text{m}^3$  and length greater than 18,000  $\mu\text{m}$**

- i. In the *LMSearch* panel, *Add Volume* and *Length* from the top left metric list. In the top right window, where both functions appear, select *Total\_Sum* as *Metric*, the symbol *>* as *Operator*, and the respective numerical values as in the heading of this use case.
- ii. To load all the CA1 neurons of Amaral’s archive, click *Choose File* and select the “*AmaralOrigCA1*” directory. Upon hitting *Start Search*, the results appear as in Figure 6.

**(H) Statistical analysis of search results**

- i. Perform the steps described in Case G, and then within the *LMSearch* panel, click *Load to Group1*.
- ii. Repeat the search of Case G, with the following alternative criteria: *Volume* less than  $2000 \mu\text{m}^3$  OR *Length* less than  $18000 \mu\text{m}^3$ . To do so, the only steps to change are the selection of the *Connector* as *OR* for the second function in the right list of the *LMSearch* panel, and the use of the  $<$  symbol under *Operator* for both functions. After executing the search, select *Load to Group2* (if the button cannot be found, enlarge the window).
- iii. In the *Specificity* panel, select *Type* from left list. Press the *Add* button.
- iv. Set  $=$  as *Operator*. Input 4 in the *Value* cell.
- v. Select *Type* from left list. Press the *Add* button.
- vi. Set *OR* for the second row *Connector* and  $=$  as *Operator*. Input 3 for *Value*.
- vii. Go to *Input* tab, check *Stat\_tests* to enable the statistical comparison analysis. Also, select *Wilcoxon* from *Tests* and *Bonferroni* from *Corrections*.
- viii. Switch to the *Function* tab, check *Stat\_tests*, and select *Terminal\_degree*, *Branch\_Order*, *Bif\_tilt\_local* (local bifurcation tilt angle), and *Rall\_Power* metrics. Click the *Add* button, making sure that all 4 metrics appear in the top left window. Select *Max* for *Terminal\_degree* and *Branch\_Order*, and *Avg* for *Bif\_tilt\_local* and *Rall\_Power*.
- ix. In the *Go* tab, click the *Go* button. The results will appear as in Table 4.

**(I) Tabulating surface area in basal dendrites farther than two bifurcations away from the soma as a function of relative path distance in individual subtrees**

- i. In the *Specificity* panel, select *Type* from left list. Press the *Add* button.
- ii. Set  $=$  as *Operator*. Input 3 for *Value* cell.
- iii. Select *Branch Order* from left panel and press *Add*. Set *AND* as *Connector* and  $>$  as *Operator*. Input 2 in *Value*.
- iv. In the *Function* panel select *Surface* from the top left metric list, and *PathDistance* from the bottom left list. Click on *Number of bins* (determining in how many equal values path distance gets subdivided) and set its value to 5 in the text box. Then, press the *Add* button.
- v. In the *Input* panel add the single cell c10261.CNG.swc from the *AmaralOrigCA1* folder.
- vi. In the *Output* panel, mark the *Subtrees Group* box, and check the *Analyze Subtrees* option.
- vii. Finally, hit the *Go* button in the *Go* panel. In this case, only 3 subtrees satisfy the *Specificity* criteria, as presented in Table 5.

## TIMING

All the examples explained in previous sections can be executed on both local and on-line version of LM. The on-line LM tool response time varies between few seconds to few minutes. For small number of input files (1–3), the output is given almost immediately. If the files are more than 10, then a response time between 1–2 minutes is normal. A statistical test between two groups, each with 10–25 neurons, would take 2 minutes of time. It is preferable to use the standalone version of LM for all computationally heavy tasks such as statistical tests, subtree analysis, and morphological searches. The online LM loading time is between 1–2 minutes depending upon the underlying RAM capacity of the machine and its Internet connection speed.

## ?TROUBLESHOOTING

- When running the standalone version, if the graphical user interface fails to show up by double clicking the Lm.jar icon, use the command line `java -jar Lm.jar` instead.
- An official LM support list server provides assistance to LM users in terms of technical and scientific questions (e-mail: l-measure-software-support-list@googlegroups.com).

## ANTICIPATED RESULTS

At this stable and mature stage of development, LM strives to balance an intuitive and user-friendly design with a flexible execution of the measurement operations. With moderate practice, users can exploit the most sophisticated options of single-cell morphometry in just a few clicks. The dual availability of LM online and as a downloadable executable allows both an agile use through a standard web browser and the incorporation of the morphometric functionality in scripted batch processes and arbitrary manipulations of the results. In addition to the user documentation, a web-accessible and email-based support group is also active. Future additions and upgrades will be prioritized on the basis of the community requests.

The 8 protocols presented do not exhaustively cover all LM functionality, but show a range of potential applications. For example, Tables 2–5 report the results of morphological analysis carried out on multiple neurons, lending themselves to a direct interpretation. In Table 2, the two cells present total cable lengths of 13257.7  $\mu\text{m}$  and 13044.9  $\mu\text{m}$ , respectively. For the first neuron (c11563.CNG.swc), the distance between two consecutive tracing points averages 14.21  $\mu\text{m}$  ( $\pm 6.42$ ), ranging from 1.12 to 42.51  $\mu\text{m}$  over 933 data points. In Table 3 two groups of neurons, one with 23 cells and the other with 24, are statistically compared with respect to length, surface, and branch order. Only the difference in the average value of branch order is statistically significant between the two groups. Similarly, Table 4 presents the comparative analysis of two other groups of neurons selected based on a morphometric search. Results show statistical difference only for the average value of Rall's power. Finally, Table 5 shows results relating surface area to path distance for the 3 basal dendrites of an individual neuron.

With minimal practice, simple variations of the above options will enable the reader to reproduce, alter, and enhance the data displayed in the four panels of Figure 3, which were plotted with MS-Excel after saving the results on the local hard drive as .xls file via the *Output File* button in the *Output* panel.

## Acknowledgments

This research was supported by NIH R01 grant NS39600 jointly funded by NINDS, NIMH, and NSF under the Human Brain Project.

## References

1. Ascoli GA, Krichmar JL, Nasuto SJ, Senft SL. Generation, description and storage of dendritic morphology data. *Philos Trans R Soc Lond B Biol Sci.* 2001; 356:1131–1145. [PubMed: 11545695]
2. Pyapali GK, Turner DA. Increased dendritic extent in hippocampal CA1 neurons from aged F344 rats. *Neurobiol Aging.* 1996; 17:601–611. [PubMed: 8832635]
3. Bulinski JC, et al. Changes in dendritic structure and function following hippocampal lesions: correlations with developmental events? *Prog Neurobiol.* 1998; 55:641–650. [PubMed: 9670222]
4. Cannon RC, Wheal HV, Turner DA. Dendrites of classes of hippocampal neurons differ in structural complexity and branching patterns. *J Comp Neurol.* 1999; 413:619–633. [PubMed: 10495447]
5. Ascoli GA. Neuroanatomical algorithms for dendritic modelling. *Network.* 2002; 13:247–260. [PubMed: 12222813]
6. Migliore M, Ferrante M, Ascoli GA. Signal propagation in oblique dendrites of CA1 pyramidal cells. *J Neurophys.* 2005; 94:4145–4155.
7. Turner, DA.; Cannon, RC.; Ascoli, GA. Web-based neuronal archives: neuronal morphometric and electrotonic analysis. In: Kotter, R., editor. *Neuroscience databases.* Boston: Kluwer Academic Publishers; 2002. p. 81-98.
8. Ascoli GA. Mobilizing the base of neuroscience data: the case of neuronal morphologies. *Nature Rev Neurosci.* 2006; 7:318–324. [PubMed: 16552417]
9. Cannon RC, Turner DA, Pyapali GK, Wheal HV. An on-line archive of reconstructed hippocampal neurons. *J Neurosci Methods.* 1998; 84:49–54. [PubMed: 9821633]
10. Claiborne BJ, Amaral DG, Cowan WM. Quantitative three dimensional analysis of granule cell dendrites in the rat dentate gyrus. *J Comp Neurol.* 1990; 302:206–219. [PubMed: 2289972]
11. Henze DA, Cameron WE, Barrionuevo G. Dendritic morphology and its effects on the amplitude and rise-time of synaptic signals in hippocampal CA3 pyramidal cells. *J Comp Neurol.* 1996; 369:331–344. [PubMed: 8743416]
12. Ishizuka N, Cowan WM, Amaral DG. A quantitative analysis of the dendritic organization of pyramidal cells in the rat hippocampus. *J Comp Neurol.* 1995; 362:17–45. [PubMed: 8576427]
13. Pyapali GK, Sik A, Penttonen M, Buzsaki G, Turner DA. Dendritic properties of hippocampal CA1 pyramidal neurons in the rat: intracellular staining in vivo and in vitro. *J Comp Neurol.* 1998; 391:335–352. [PubMed: 9492204]
14. Turner DA, Li XG, Pyapali GK, Ylinen A, Buzsaki G. Morphometric and electrical properties of reconstructed hippocampal CA3 neurons recorded in vivo. *J Comp Neurol.* 1995; 356:580–594. [PubMed: 7560268]
15. Scorcioni R, Ascoli GA. Algorithmic extraction of morphological statistics from electronic archives of neuroanatomy. *Lect Notes Comp Sci.* 2001; 2084:30–37.
16. Ascoli GA, Donohue DE, Halavi M. NeuroMorpho.Org: a central resource for neuronal morphologies. *J Neurosci.* 2007; 27:9247–9251. [PubMed: 17728438]
17. Scorcioni R, Lazarewicz MT, Ascoli GA. Quantitative morphometry of hippocampal pyramidal cells: differences between anatomical classes and reconstructing laboratories. *J Comp Neurol.* 2004; 473:177–93. [PubMed: 15101088]

18. Krichmar J, Velasquez D, Ascoli GA. Effects of beta-catenin on dendritic morphology and simulated firing patterns in cultured hippocampal neurons. *Biol Bull.* 2006; 211:31–43. [PubMed: 16946239]
19. Li Y, Brewer D, Burke RE, Ascoli GA. Developmental changes in spinal motoneuron dendrites in neonatal mice. *J Comp Neurol.* 2005; 483:304–317. [PubMed: 15682391]
20. Duque A, Tepper J, Detari L, Ascoli G, Zaborszky L. Morphological characterization of electrophysiologically identified basal forebrain neurons: cholinergic vs. neuropeptide Y-containing neurons. *Brain Struct Funct.* 2007; 1:55–73. [PubMed: 17717698]
21. Brown K, Donohue D, D'Alessandro G, Ascoli GA. A cross-platform freeware tool for digital reconstruction of neuronal arborizations from image stacks. *Neuroinformatics.* 2005; 3:343–360. [PubMed: 16284416]
22. Scorcioni R, Ascoli GA. Algorithmic reconstruction of complete axonal arborizations in rat hippocampal neurons. *Neurocomputing.* 2005;65–66. 15–22.
23. Donohue D, Ascoli GA. Local diameter fully constrains dendritic size in basal but not apical trees of CA1 pyramidal neurons. *J Comput Neurosci.* 2005; 19:223–238. [PubMed: 16133820]
24. Samsonovich A, Ascoli GA. Statistical determinants of dendritic morphology in hippocampal pyramidal neurons: a hidden Markov model. *Hippocampus.* 2005; 15:166–183. [PubMed: 15390156]
25. Rodriguez A, Ehlenberger DB, Hof PR, Wearne SL. Rayburst sampling, an algorithm for automated three-dimensional shape analysis from laser scanning microscopy images. *Nat Protoc.* 2006; 1:2152–2161. [PubMed: 17487207]
26. Cannon RC, Howell FW, Goddard NH, De Schutter E. Non-curved distributed databases for experimental data and models in neuroscience. *Network: Comput Neural Syst.* 2002; 13:415–428.
27. Zheng J, et al. Classification of HIV-1-mediated neuronal dendritic and synaptic damage using multiple criteria linear programming. *Neuroinformatics.* 2004; 2(3):303–26. [PubMed: 15365193]
28. Graham JW, Jung R. Modeling morphological changes in spinal motoneurons following spinal cord injury to explore changes in electrical behavior. *BMC Neuroscience.* 2007; 8(S2):1471–2202.
29. Liebmann L, et al. Differential effects of corticosterone on the sAHP in the basolateral amygdala and CA1 region: Possible role of calcium channel subunits. *J Neurophysiol.* 2007 in press.
30. Ascoli, GA., et al. Petilla Terminology: Nomenclature of features of GABAergic interneurons of the cerebral cortex. (2008, submitted by editorial invitation to *Nature Rev. Neurosci.*, see also [www.columbia.edu/cu/biology/faculty/yuste/petilla](http://www.columbia.edu/cu/biology/faculty/yuste/petilla))
31. Uylings HBM, van Pelt J. Measures for quantifying dendritic arborizations. *Network: Comput Neural Syst.* 2002; 13:397–414.
32. Gulyás AI, Megías M, Emri Z, Freund TF. Total Number and Ratio of Excitatory and Inhibitory Synapses Converging onto Single Interneurons of Different Types in the CA1 Area of the Rat Hippocampus. *J Neurosci.* 1999; 19:10082–10097. [PubMed: 10559416]
33. Mott DD, Turner DA, Okazaki MM, Lewis DV. Interneurons of the Dentate-Hilus Border of the Rat Dentate Gyrus: Morphological and Electrophysiological Heterogeneity. *J Neurosci.* 1997; 17:3990–4005. [PubMed: 9151716]
34. Krimer LS, et al. Cluster Analysis-Based Physiological Classification and Morphological Properties of Inhibitory Neurons in Layers 2–3 of Monkey Dorsolateral Prefrontal Cortex. *J Neurophysiol.* 2005; 94:3009–3022. [PubMed: 15987765]
35. Dumitriu D, Cossart R, Huang J, Yuste R. Correlation Between Axonal Morphologies and Synaptic Input Kinetics of Interneurons from Mouse Visual Cortex. *Cereb Cortex.* 2007; 17:81–91. [PubMed: 16467567]
36. Kong JH, Fish DR, Rockhill RL, Masland RH. Diversity of ganglion cells in the mouse retina: Unsupervised morphological classification and its limits. *J Comp Neurol.* 2005; 489:293–310. [PubMed: 16025455]
37. Toris CB, Eiesland JL, Miller RF. Morphology of ganglion cells in the neonatal tiger salamander retina. *J Comp Neurol.* 1995; 352:535–559. [PubMed: 7721999]
38. da Costa LF, Velte TJ. Automatic Characterization and Classification of Ganglion Cells from the Salamander Retina. *J comp Neurol.* 1999; 404:33–51. [PubMed: 9886023]

39. Watson KK, Jones TK, Allman JM. Dendritic architecture of the von Economo neurons. *Neuroscience*. 2006; 141:1107–1112. [PubMed: 16797136]
40. Hayes TL, Lewis DA. Magnopyramidal neurons in the anterior motor speech region. Dendritic features and interhemispheric comparisons. *Arch Neurol*. 1996; 53:1277–1283. [PubMed: 8970455]
41. Sultan F, Bower JM. Quantitative Golgi study of the rat cerebellar molecular layer interneurons using principal component analysis. *J Comp Neurol*. 1998; 393:353–373. [PubMed: 9548555]
42. Weaver CM, Wearne SL. Neuronal Firing Sensitivity to Morphologic and Active Membrane Parameters. *PLoS Comput Biol*. 2008;4. in press.
43. Vetter P, Roth A, Häusser M. Propagation of Action Potentials in Dendrites Depends on Dendritic Morphology. *J Neurophysiol*. 2001; 85:926–937. [PubMed: 11160523]
44. Golding NL, Kath WL, Spruston N. Dichotomy of Action-Potential Backpropagation in CA1 Pyramidal Neuron Dendrites. *J Neurophysiol*. 2001; 86:2998–3010. [PubMed: 11731556]
45. Bui TV, Cushing S, Dewey D, Fyffe RE, Rose PK. Comparison of the Morphological and Electrotonic Properties of Renshaw Cells, Ia Inhibitory Interneurons, and Motoneurons in the cat. *J Neurophysiol*. 2003; 90:2900–2918. [PubMed: 12878716]
46. Yu X, Malenka RC.  $\beta$ -catenin is critical for dendritic morphogenesis. *Nat Neurosci*. 2003; 6:1169–1177. [PubMed: 14528308]
47. Vyas A, Mitra R, Rao BSS, Chattarji S. Chronic Stress Induces Contrasting Patterns of Dendritic Remodeling in Hippocampal and Amygdaloid Neurons. *J Neurosci*. 2002; 22:6810–6818. [PubMed: 12151561]
48. Maravall M, Koh IYY, Lindquist WB, Svoboda K. Experience-dependent Changes in Basal Dendritic Branching of Layer 2/3 Pyramidal Neurons During a Critical Period for Developmental Plasticity in Rat Barrel Cortex. *Cereb Cortex*. 2004; 14:655–664. [PubMed: 15054062]
49. Marks WB, Burke RE. Simulation of motoneuron morphology in three dimensions. I. Building individual dendritic trees. *J Comp Neurol*. 2007; 503:685–700. [PubMed: 17559104]
50. Weaver CM, Hof PR, Wearne SL, Lindquist WB. Automated algorithms for multiscale morphometry of neuronal dendrites. *Neural Comput*. 2004; 16:1353–1383. [PubMed: 15165394]
51. Sholl DA. Dendritic organization in the neurons of the visual and motor cortices of the cat. *J Anat*. 1953; 87:387–406. [PubMed: 13117757]



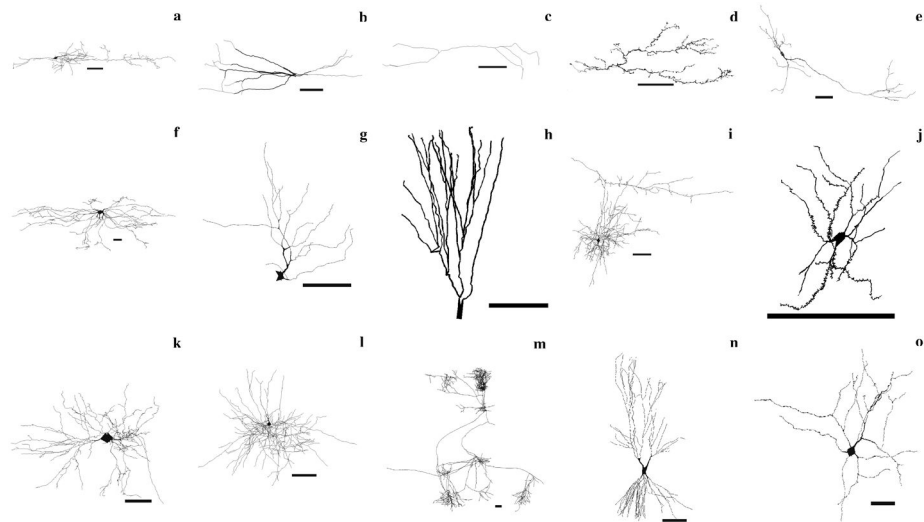


**Figure 1.**

Representative collection of 15 neurons selected from NeuroMorpho.Org (all scale bars are 100  $\mu\text{m}$ ). Ordered by row, from top left: (a) bipolar cell from rat neocortex (C130200-19), (b) parvalbumin cell from rat hippocampus (pv22c), (c) calretinin cell from rat hippocampus (cr10f), (d) climbing fiber from rat cerebellum (NMA), (e) dopaminergic cell from rat basal ganglia (Nigra11h941-1), (f) dorsal spinocerebellar tract cell from cat spinal cord (DSCT4), (g) ganglion cell from salamander retina (mp\_ma\_40984\_gc2), (h) granule cell from rat hippocampus (411884b), (i) Martinotti cell from rat cerebral cortex (cellC150897B-I1), (j) medium spiny neuron from mouse basal forebrain (ACC1), (k) motoneuron from mouse spinal cord (ok\_m215), (l) basket cell from rat neocortex (C040600B1), (m) pyramidal cell from cat neocortex (980804axden), (n) CA3 pyramidal cell from rat hippocampus (cell6zr), (o) Renshaw cell from cat spinal cord (renshawcell1).

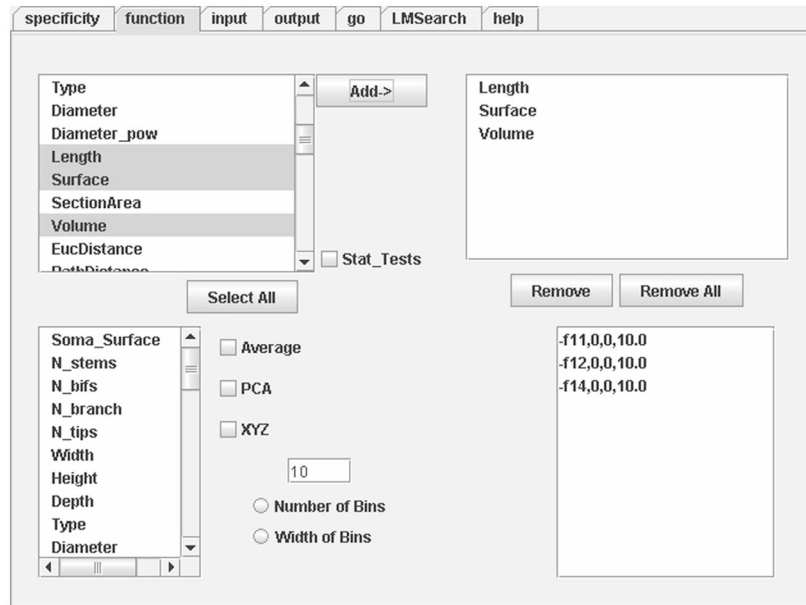


**Figure 2.**  
 In the Function tab users define the metrics to extract. Detailed definition of each metric is available in the Help panel (which also provides general usage information).

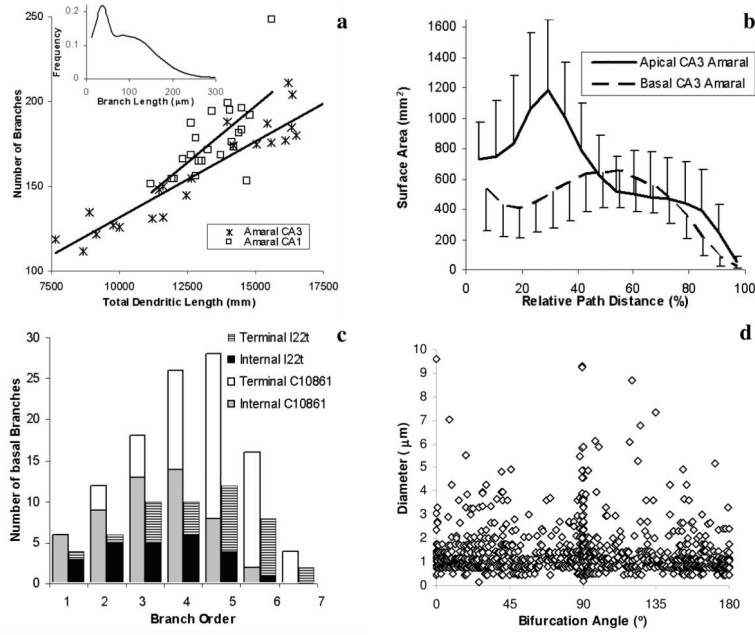


**Figure 3.** Examples of graphs from typical morphometric studies performed with LM on reconstructed neurons available at NeuroMorpho.Org. (a) Scatter plot of the overall number of branches in each cell vs. its total dendritic length. Straight lines represent linear fits. Inset shows frequency distribution of Branch Length for all Amaran CA3 group. (b) Distributions of surface area over relative path distance for apical and basal dendrites from CA3 pyramidal cell from Amaran archive. Each point is the average over 24 cells, error bars represent standard deviations. (c) Histograms of the number of basal branches (divided in internal, i.e. ending into a bifurcation, and terminal, i.e. ending into a tip) as a function of branch order (the number of bifurcations from the soma) for CA3 pyramidal cells I22t and c10861. (d) Scatter plot of diameter vs. bifurcation angle for each branch point within all 18 CA3 pyramidal neurons from young rats in Turner’s archive. Artificial noise uniformly distributed between  $-0.05$  and  $0.05$  was added to all coordinate values for better visualization.

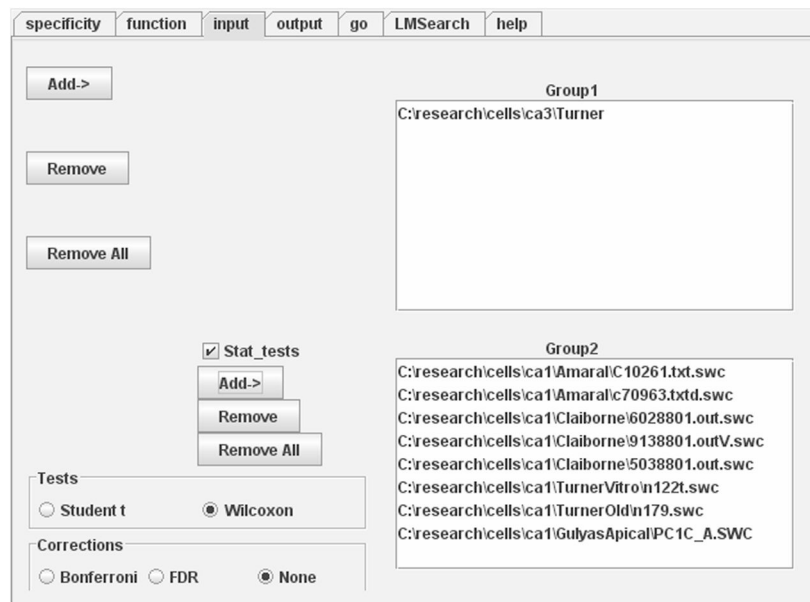


**Figure 4.** Input panel with statistical feature enabled (note “Stat\_tests” checkbox). All cells from directory \ca3\Turner are loaded as Group1, while eight neurons from five different directories are pooled into Group2. The Input panel identifies the cells to be analyzed, while the Output tab determines if and where the results should be saved to disk.

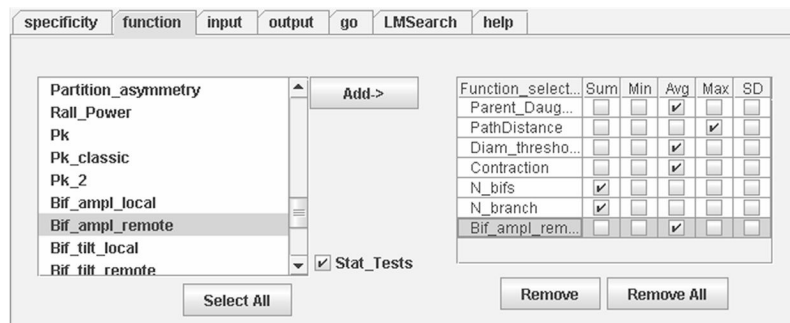


**Figure 5.** Function panel with statistical features enabled (note “Stat\_tests” checkbox). After the morphometric analysis conditions are set, extraction of measurements is initiated in the Go panel.

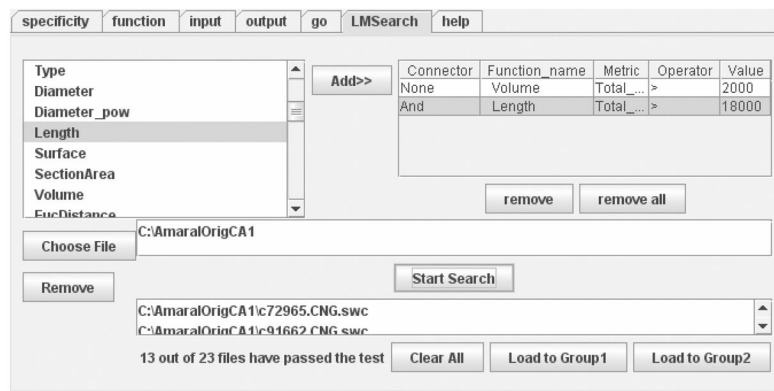


**Figure 6.**

The LMSearch panel allows users to find neuronal reconstructions with particular morphometric characteristics among arbitrarily large sets. In this example, the search criteria indicate a Total Length greater than 18000  $\mu\text{m}$  and a Total Volume greater than 2000  $\mu\text{m}^3$ . The resulting output consists of 13 neurons that satisfy these conditions over a total of 23 contained in AmaralOrigCA1 folder.

**Table 1**

Partial list of LM metrics (the unit for all dimensional values is  $\mu\text{m}$ ). All metrics return real values unless otherwise noted. Metrics in the left column return values at each tracing point except the gray shaded ones, which are defined at the whole neuron level. Metrics in the right column return one value for every branch, except the gray shaded ones, which are defined at bifurcation points only.

Somatic Surface	Branch Length
Neuronal Height	Contraction
Neuronal Width	Fragmentation <sup>(2)</sup>
Neuronal Depth	Fractal dimension
Diameter	Branch Taper
Distance from previous point	Daughter Diameter Ratio
Unit Taper	Parent/Daughter Ratio
Euclidian Distance from Soma	Rall Power
Path Distance from Soma	Rall Ratio
Branch Origin <sup>(1)</sup>	Power Ratio
Branch Ending <sup>(1)</sup>	Partition Asymmetry
Branch Order <sup>(2)</sup>	Local Amplitude Angle
Type <sup>(2)</sup>	Remote Amplitude Angle
Terminal Degree <sup>(2)</sup>	Local Tilt Angle
Helix	Remote Tilt Angle
	Local Torque Angle
	Remote Torque Angle

<sup>(1)</sup> Returns binary values (1 or 0, i.e. “Yes” or “No”).

<sup>(2)</sup> Returns integer values.

**Table 2**

Output of case B. Each line can be read from right to left as: neuron name, metric function, total sum of the function over all tracing points, number of points included in the analysis, number of points excluded (in this case, around 400 points define the cell body, fiduciary axis, axons, etc), minimum value, average, maximum, and standard deviation of the metric function.

Neuron Name	Metric	TotSum	P.In	P.Ex	Min	Avg	Max	Std
c11563.CNG.swc	Length	13257.7	933	-410	1.12	14.21	42.51	6.42
c11563.CNG.swc	Surface	13275.9	933	-410	1.05	14.23	117.62	8.48
c11563.CNG.swc	Volume	1187.16	933	-410	0.08	1.27	73.13	3
c10261.CNG.swc	Length	13044.9	1305	-404	1.12	10	33.67	5.43
c10261.CNG.swc	Surface	14951.9	1305	-404	1.4	11.46	294.79	11.27
c10261.CNG.swc	Volume	2153.41	1305	-404	0.11	1.65	316.9	9.43



**Table 3**

Output of case F. Each line can be read from right to left as metric function, Statistic, sample size for Group1, mean value for Group1, standard deviation for Group1, sample size for Group2, mean value for Group2, standard deviation for Group2, p-value for Wilcoxon test, p-value corrected with Bonferroni.

Function_name	Statistic	N1	Mean1	SD1	N2	Mean2	SD2	Wilcoxon P_Values	Bonferroni correction
Length	Sum	23	13475.14	1095.79	24	13196.08	3149.861	0.45	>=1
Surface	Sum	23	14811.28	1566.22	24	18587.15	6153.017	0.02	0.062
Branch_Order	Avg	23	9.65	1.87	24	13196.08	3149.861	2.14E-09	6.41E-09

**Table 4**

Output of case H. Each line can be read from right to left as metric function, Statistic, sample size in Group1, mean value for Group1, standard deviation for Group1, sample size in Group2, mean value for Group2, standard deviation for Group2, p-value for Wilcoxon test, p-value corrected with Bonferroni.

Function_name	Statistic	N1	Mean1	SD1	N2	Mean2	SD2	Wilcoxon P_Values	Bonferroni correction
Bif_tilt_local	Avg	13	131.42	3.8	10	132.17	4.34	0.38	>=1
Rall_Power	Avg	13	1.18	0.2	10	1.44	0.14	0.002	0.01
Terminal_degree	Max	13	55.15	13.06	10	57.3	8.86	0.39	>=1
Branch_Order	Max	13	24.23	5.61	10	25.9	4.28	0.18	0.74

**Table 5**

Output of case I. Tabulating Surface Area versus Path Distance for the 3 basal sub trees of neuron c10261. Each line can be read from right to left as neuronal tree name, followed by the two tabulated metrics. The V values represent the extracted measures for the 5 bins (e.g. V1: first value for bin 1).

Tree Name	Metric	V1	V2	V3	V4	V5	V6
c10261.CNGtree4.swc	PathDistance	112.7	142.09	171.48	200.87	230.26	259.65
	Surface	26.87	58.51	68.67	90.5	67.42	16.03
c10261.CNGtree2.swc	PathDistance	60.07	108.22	156.36	204.51	252.65	300.8
	Surface	71.4	305.64	403.86	459.72	264.7	93.57
c10261.CNGtree6.swc	PathDistance	84.02	126.05	168.09	210.13	252.16	294.2
	Surface	51.37	162.17	254.11	339.39	211.77	25.36